Published in final edited form as:
Neuron. 2012 April 12; 74(1): 136–150. doi:10.1016/j.neuron.2012.01.029.

Identification of CSPα clients reveals a role in dynamin 1 regulation

Yong-Quan Zhang[1,7], **Michael X. Henderson**[1,7], **Christopher M. Colangelo**[3], **Stephen D. Ginsberg**[5], **Can Bruce**[3,4], **Terence Wu**[3], and **Sreeganga S. Chandra**[1,2,6]

[1]Program in Cellular Neuroscience, Neurodegeneration and Repair, Dept. of Neurology, Yale University, New Haven, CT 06536

[2]Dept. of Molecular Cell and Developmental Biology, Yale University, New Haven, CT 06536

[3]W. M. Keck Foundation Biotechnology Resource Laboratory, Mass Spectrometry Resources, Yale University, New Haven, Connecticut 06510

[4]Dept. of Molecular Biophysics and Biochemistry, Yale University, New Haven, Connecticut 06510

[5]Center for Dementia Research, Nathan Kline Institute and Department of Psychiatry, New York, University Langone Medical Center, New York, NY 10962

SUMMARY

Cysteine string protein α (CSPα), a presynaptic co-chaperone for Hsc70, is required for synapse maintenance. Deletion of CSPα leads to neuronal dysfunction, synapse loss, and neurodegeneration. We utilized unbiased, systematic proteomics to identify putative CSPα protein clients. We found 22 such proteins whose levels are selectively decreased in CSPα knockout synapses. Of these putative CSPα protein clients, two directly bind to the CSPα chaperone complex and are bona fide clients. They are the t-SNARE SNAP-25 and the GTPase dynamin 1, which are necessary for synaptic vesicle fusion and fission, respectively. Using hippocampal cultures, we show CSPα regulates the stability of client proteins and synaptic vesicle number. Our analysis of CSPα-dynamin 1 interactions reveals unexpectedly that CSPα regulates the polymerization of dynamin 1. CSPα therefore participates in synaptic vesicle endocytosis and may facilitate exo- and endocytic coupling. These findings advance the understanding of how synapses are functionally and structurally maintained.

INTRODUCTION

Synapses need to be functionally and structurally maintained throughout life to preserve stable neuronal networks and normal behavior (Holtmaat and Svoboda, 2009; Lin and Koleske, 2010). Longitudinal *in vivo* imaging in mice has shown that the majority of synapses are stable for a lifetime (Grutzendler and Gan, 2006; Holtmaat et al., 2006). In contrast, the loss of synapses appears to be an early, pathogenic event in neurodegenerative diseases such as Alzheimer's and Parkinson's disease (Nikolaus et al., 2009; Selkoe, 2002).

[6]To whom correspondence should be addressed. Tel. 203-785-6172, Fax 203-737-1761, sreeganga.chandra@yale.edu.
[7]These authors contributed equally to this study.

These findings suggest that normal synaptic maintenance mechanisms are disrupted in these diseases.

CSPα (*Dnajc5*) is a presynaptic co-chaperone that is vital for presynaptic proteostasis and synapse maintenance (Chandra et al., 2005; Fernandez-Chacon et al., 2004; Garcia-Junco-Clemente et al., 2010; Tobaben et al., 2001). CSPα binds the heat shock protein cognate 70 (Hsc70) and the tetratricopeptide protein SGT to form a functional chaperone complex on synaptic vesicles (Braun et al., 1996; Chamberlain and Burgoyne, 1997a,;Evans et al., 2003; Johnson et al., 2010; Tobaben et al., 2001; Zinsmaier and Bronk, 2001). CSPα contains highly conserved domains. These include an N-terminal J-domain characteristic of the DnaJ/Hsp40 cochaperone family that activates the ATPase activity of Hsc70 (Braun et al., 1996; Chamberlain and Burgoyne, 1997a), a middle cysteine string domain with 11 to 13 cysteines which are palmitoylated and critical for binding to synaptic vesicles (Greaves and Chamberlain, 2006; Ohyama et al., 2007), and a C-terminus which binds SGT and Hsc70 clients (Tobaben et al., 2001). In keeping with its relevance to synaptic function, CSPα is broadly expressed in the nervous system.

A loss-of-function CSP mutant in *Drosophila* exhibits a temperature-sensitive transmitter release defect and early lethality (Umbach et al., 1994; Zinsmaier et al., 1994). Similarly, deletion of CSPα in mice causes progressive defects in neurotransmission, synapse loss, degeneration, and early lethality (Chandra et al., 2005; Fernandez-Chacon et al., 2004). Synaptic deficits in the CSPα KO commence around postnatal day 20 (P20) and the accruing loss of synapses renders the mice moribund by P40. Interestingly, synapse loss in the CSPα KO is activity-dependent, i.e. synapses that fire more frequently are lost first (Garcia-Junco-Clemente et al., 2010; Schmitz et al., 2006). These *in vivo* phenotypes strongly suggest that CSPα acts to maintain synapses. However, the CSPα-dependent mechanisms that confer synapse protection are unclear.

Initial experiments in fly suggested that CSP participates directly in synaptic vesicle exocytosis by binding to calcium channels or the G α_s protein, which in turn blocks calcium channels (Gundersen and Umbach, 1992; Leveque et al., 1998; Magga et al., 2000). However, later biochemical findings unequivocally demonstrated that CSPα forms a chaperone complex with Hsc70 and SGT on synaptic vesicles (Tobaben et al., 2001). This indicated that CSPα may regulate the synaptic vesicle cycle through refolding or switching the conformation of proteins necessary for the cycle. In fact, CSPα KO mice show no defect in calcium or neurotransmitter release at P10, but do show such synaptic deficits by age P20 (Fernandez-Chacon et al., 2004; Garcia-Junco-Clemente et al., 2010). These results strongly suggest that with repeated firing and multiple rounds of the synaptic vesicle cycle, CSPα KO synapses likely accrue incorrect conformations of CSPα clients, eventually leading to synaptic dysfunction and loss.

Recent biochemical analyses of CSPα KO mice showed that the t-SNARE SNAP-25 is a protein substrate or client of the Hsc70-CSPα chaperone complex and that deletion of CSPα leads to a 50% decrease in SNAP-25 levels (Chandra et al., 2005; Sharma et al., 2011). Nonetheless, SNAP-25 heterozygous mice, which also have a similar decrease in SNAP-25 levels and function, are phenotypically normal (Washbourne et al., 2002), suggesting other unknown client proteins contribute to the CSPα KO phenotypes. Identification of these clients is critical to understanding CSPα-dependent mechanisms of synapse maintenance. The decrease of SNAP-25 levels in CSPα KO brains suggests that misfolded clients are degraded and that additional clients can be screened for on the basis of lowered synaptic protein amounts in CSPα KO brains. It should be noted that several proteins that bind CSPα have been identified in different model systems, including the SNARE syntaxin, G α_s, rab3b, and synaptotagmin 9 (Boal et al., 2011; Magga et al., 2000; Natochin et al., 2005; Nie

et al., 1999; Sakisaka et al., 2002), but none of these proteins have been unambiguously demonstrated to be clients of the Hsc70-CSPα chaperone complex.

In this study, we use unbiased, systematic proteomics to identify CSPα client proteins and show that SNAP-25 and the endocytic GTPase dynamin 1 are key clients of the Hsc70-CSPα chaperone complex. We additionally demonstrate that CSPα promotes the self-assembly of dynamin 1, thereby regulating synaptic vesicle endocytosis. Finally, we show that the levels of CSPα chaperone complex are decreased in Alzheimer's disease brains. Our results reveal that CSPα participates in an essential presynaptic quality control mechanism that allows for the activity-dependent maintenance of synapses.

RESULTS

Proteomic Screen for CSPα Clients Identifies Key Exo- and Endocytic Proteins

Chaperones are critical for protein homeostasis and help refold non-native proteins and allow for conformational switches of folded proteins (Fujimoto and Nakai, 2010; Voisine et al., 2010). In their absence, misfolded proteins are either targeted for degradation or form aggregates, leading to a decrease in native protein amounts. We therefore hypothesized that the levels of CSPα clients should be reduced in CSPα KO brains. To identify the repertoire of CSPα clients in the presynaptic terminal, we performed an unbiased quantitative comparison of the synaptic proteomes of wildtype and CSPα KO brains. We employed two proteomic methods—DIGE (2-D fluorescence Difference Gel Electrophoresis) and iTRAQ (Isobaric Tag for Relative and Absolute Quantitation). DIGE and iTRAQ use differential tags, fluorescent and isobaric respectively, to monitor protein changes (Tannu and Hemby, 2006) and are used in a complementary fashion. We chose to perform these experiments at postnatal day 28 (P28) because synaptogenesis is mostly complete at this time and synapse loss in CSPα KOs is not yet pronounced (Chandra et al., 2005; Fernandez-Chacon et al., 2004). This time point therefore avoids non-specific changes in synaptic proteins that occur once more synapses are lost in CSPα KO mice.

Wildtype and CSPα KO brains were homogenized to prepare synaptosomes and further fractionated to obtain purified synaptic plasma membranes, cytosol, and synaptic vesicles (Fig. 1A). This fractionation procedure allowed us to increase our signal-to-noise ratio and delve deeper into the synaptic proteome. The synaptic plasma membrane, cytosol, and vesicle fractions of the two genotypes were subjected to DIGE and iTRAQ in a pair-wise fashion. We carried out multiple independent DIGE and iTRAQ experiments, and analyzed over 1500 synaptic proteins in the three fractions (Table I). By analyzing these ~1500 proteins, we sampled nearly the entire synaptic proteome. All protein changes over 40% were scored and identified by mass spectrometry. Fig. 1B shows a DIGE experiment on the synaptic plasma membrane fraction of wildtype and CSPα KO brains. The gels revealed only a few protein changes between the two genotypes, supporting our hypothesis that deletion of CSPα leads initially only to the loss of its clients. Similar to the DIGE runs, the iTRAQ experiments also showed select changes in protein levels (Fig. 1C, S1). The most prominent changes were, as expected, for CSPα and for the t-SNARE SNAP-25 (Fig. 1B–C; S1A, C), the previously characterized CSPα client (Chandra et al., 2005; Sharma et al., 2011), validating this approach to identify other CSPα clients.

We considered a synaptic protein to be a potential CSPα client if its levels were changed significantly in CSPα KO samples in at least two independent proteomic experiments. Based on these stringent criteria, we identified a total of 37 proteins (Table I). This set of candidate client proteins has striking features: 1) Most of the identified proteins are presynaptic, as opposed to postsynaptic, as would be expected for CSPα clients. 2) The putative clients include known physical and genetic interactors of CSPα, such as Hsc70, SNAP-25, α- and -

synucleins (Chandra et al., 2005). 3) For certain proteins, such as dynamin 1, we see a redistribution of the protein's subcellular localization (Fig. S2A–B). 4) We observed a pronounced decrement of other components of the cytosolic Hsc70 chaperone network such as Stip 1/HOP, Hip, and Hsp90, affirming that deletion of Hsp40s destabilizes chaperone complexes (Sahi and Craig, 2007). 5) Besides chaperones, we identified five other classes of proteins: exocytic, endocytic, cytoskeletal, signaling, and other synaptic proteins. Consistent with this identification, the following Gene Ontology molecular function terms were enriched-- unfolded protein binding ($p = 1.5$ e-10), chaperone binding ($p = 3.1$ e-6), SNARE binding ($p = 1.5$ e-4), GTP binding ($p = 2.9$ e-4), and cytoskeletal pathways ($p = 1.1$ e-3), signifying that these functions are perturbed in CSPα KO synapses (Table S1).

The 27 proteins we identified in our proteomic screen, besides the 10 chaperones, are potential CSPα clients (Table I). These include exocytic proteins that are components of the SNARE machinery (SNAP-25, complexin I, NSF) and endocytic proteins that regulate vesicle fission (dynamin 1, Necap 1). Cytoskeletal proteins include regulators of the actin and microtubule cytoskeleton (Crmp2, Crmp3, and BASP1) and GTP binding cytoskeletal proteins (Septin 3, 5, 6, and 7). Many of these proteins are represented in Gene Ontology shortest pathway networks emanating from CSPα that are linked by a maximum of three interactions (Fig. 1D), adding further credence that they may indeed be direct CSPα clients. Our proteomic analysis raises the possibility that CSPα acts on clients that participate in the synaptic vesicle cycle and/or on cytoskeletal proteins to regulate synapse function and stability.

Validation of CSPα Clients

We confirmed the protein changes in CSPα KO synapses, using two orthogonal methods. First, we performed Multiple Reaction Monitoring (MRM) on the same samples we used for the DIGE and iTRAQ experiments. This targeted, label-free proteomic method analyzes the levels of select signature peptides for a given protein and has a high signal to noise ratio (Yocum and Chinnaiyan, 2009). The MRM method is particularly useful to quantify proteins for which antibodies are not readily available. We were able to get clear MRM signals for 21 of the proteins tested. The MRM results confirmed the proteomically observed protein decreases for 17 proteins, including dynamin 1, Hsc70, Hsp70, Stip 1/HOP, Septin 3, 6, 7, α-and β-synuclein (Validation Rate = 81%; Table S2). We also showed that 4 proteins-Crmp3, Septin 5, PSD-95, and Rabconnectin 3b were unchanged in CSPα KO brains. Second, we used quantitative immunoblotting of wildtype and CSPα KO (P28) synaptosomes to verify the decreases in proteins noted in Table I. As shown in Figs. 2A–B, we confirmed most of the prominent changes observed in the DIGE and iTRAQ experiments, including for dynamin 1, SNAP-25, complexin I, BASP1, NSF, and several chaperone components. In addition, we found that the levels of Septin 5 and PSD-95 to be unchanged.

To determine if changes in CSPα client protein levels were restricted to synapses, we performed a comparable analysis using total brain homogenate from P28 wildtype and CSPα KOs. We obtained results similar to that observed in synaptosomes (Fig. S2C), in keeping with the fact that several of these proteins are mainly synaptic. For proteins that are not exclusively localized to the presynaptic terminal, such as dynamin 1 and BASP1, the decrease in protein levels was only observed in synaptosomes but not in total brain homogenates (Fig. S2C). This indicates that dynamin 1 and BASP1 are subject to CSPα-regulated quality control mechanisms only at the nerve terminal.

Collectively, by MRM and quantitative immunoblotting we experimentally verified 22 of the 37 proteins whose levels are decreased in the CSPα KO, while the levels of 4 proteins were unchanged. We consider these 22 synaptic proteins to be high confidence members of

the CSPα interactome (Table I, Validation Column). Of these proteins, 15 belong to protein classes other than chaperones.

To determine if the observed protein changes precede the synaptic dysfunction, synapse loss and neurodegenerative phenotypes of the CSPα KO, we repeated the quantitative immunoblotting analyses on synaptosomes derived from P10 mice. At this age, CSPα KOs are healthy and indistinguishable from their wildtype littermates. Figs. 2C–D show that changes in dynamin 1, SNAP-25, complexin I, BASP1 and NSF occur prior to the onset of CSPα phenotypes, suggesting these protein changes may be causal to the subsequent synapse dysfunction. Surprisingly, we did not see changes in the levels of chaperones at P10. This discrepancy is likely due to the fact that steady state levels reflect both protein synthesis and degradation and under conditions of stress, heat shock proteins are induced. For select CSPα interactome members we determined that their mRNA levels were unchanged in wildtype and CSPα KO brains, indicating that the observed decreases in protein levels occurred post-transcriptionally (Fig. S2D–E).

Identification of Dynamin 1 as a CSPα Client

The 15 proteins whose levels we validated in the CSPα KO can either be direct clients of the CSPα chaperone complex or indirectly decreased due to secondary changes. To determine which of these proteins are direct clients, we tested if they bind either CSPα or Hsc70 in a nucleotide-dependent manner. In the presence of ATP, clients typically bind the Hsc70-DnaJ co-chaperone complex with low affinity, while ADP promotes a high affinity interaction (Kampinga and Craig, 2010). We expressed CSPα and Hsc70 as GST fusions and carried out GST-pulldowns with wildtype mouse brain homogenates (Fig. 3A), using the Hsc70 binding protein Stip 1/HOP as a positive control. Our results revealed that dynamin 1 binds CSPα, suggesting it is a client of this chaperone complex. Importantly, dynamin 1 behaves like a prototypical Hsc70-DnaJ chaperone client in that it binds CSPα and not Hsc70, and its binding is ADP-dependent. Consistent with previously published work, SNAP-25 binds both CSPα and Hsc70 (Fig. 3A; (Chandra et al., 2005; Sharma et al., 2011). Additionally, we could show that BASP1 is an Hsc70 binding protein and rule out that complexin I, NSF, and synucleins are direct CSPα clients. Based on our proteomic and biochemical analysis, we narrowed our analysis of CSPα clients to dynamin 1 and SNAP-25.

We confirmed the interactions of both dynamin 1 and SNAP-25 with the CSPα chaperone complex *in vivo* by immunoprecipitating dynamin 1 and SNAP-25 with CSPα from brain homogenates in the presence of nucleotides (Fig. 3B). Again, the binding of dynamin 1, but not of SNAP-25, to CSPα, is promoted by addition of ADP. We also showed these interactions with proteins heterologously expressed in HEK 293T cells (Fig. 3C). These results indicate dynamin1 and SNAP-25 are both direct clients of the Hsc70-CSPα chaperone complex, but probably have different sites of interaction. We therefore tested binding of dynamin 1 and SNAP-25 to CSPα and Hsc70 with purified proteins. As seen in Fig 3D, dynamin 1 is recruited to this complex via CSPα binding, while SNAP-25 is recruited via Hsc70 (Sharma et al., 2011). Previous work has shown that binding of purified SNAP-25 to Hsc70 is stabilized in the presence of ADP-S (Sharma et al., 2011).

Based on these findings, we predicted that the two clients may have different effects on the nucleotide binding domain of Hsc70 and therein its ATPase activity. We assayed the effect of dynamin 1 and SNAP-25 on the ATPase activity of Hsc70. As previously published, Hsc70 has a low basal ATPase activity that can be accelerated by addition of CSPα (Fig. 3E) (Braun et al., 1996). We also tested a CSPα construct in which the HPD motif in the J-domain has been mutated to diminish Hsc70 binding ($CSP\alpha_{QPN}$). This CSPα mutant is impaired in its ability to stimulate the ATPase activity of Hsc70 and served as a negative control (Fig. 3E) (Chamberlain and Burgoyne, 1997b). We next tested the effect of client

proteins in this assay. Addition of dynamin 1 strongly accelerates the ATPase activity of Hsc70 in the presence of CSPα(Fig. 3F)however SNAP-25 has no significant effect (Fig. 3G). The distinct interactions of dynamin 1 and SNAP-25 with the Hsc70-CSPα chaperone complex mirror the diversity of Hsc70/Hsp70- DnaJ-client interactions and are consistent with other client protein interactions (DeLuca- Flaherty et al., 1990; Kaminga and Craig, 2010). As both SNAP-25 and dynamin 1 play pivotal roles in the synaptic vesicle cycle, they are highly relevant for the functional and structural maintenance of synapses.

Cultured CSPα KO Neurons Exhibit Synapse Loss and Reduced Client Levels

Cultured hippocampal neurons derived from CSPα KO mice reproduce many features observed in KO mice and are an excellent system to investigate CSPα function. CSPα KO neurons lose 28% of their synapses at 21 DIV and 72% at 28 DIV as compared to their wildtype controls (Fig. 4A–B), reflecting the progressive synapse loss in these mice, as previously reported (Garcia-Junco-Clemente et al., 2010). Immunostaining of these neurons revealed that CSPα co-localizes with client proteins SNAP-25 and dynamin 1 (Fig. S3A; Mander's coefficient Mx = 0.97 for SNAP-25 and Mx = 0.86 for dynamin 1). Quantitative immunoblotting of neuronal cultures showed that the levels of SNAP-25 were decreased while the levels of dynamin 1 and control proteins were unchanged (Fig. 4C–D). This result is congruent with our observations that dynamin 1 levels are only decreased in the synaptic fraction of CSPα KO brains (Fig. 2A–D and S2C). We also tested the effect of overexpression of CSPα in wildtype and CSPα KO neurons. Lentiviruses that express either GFP, CSPα or the $CSP\alpha_{QPN}$ mutant were used to infect neurons at 5 DIV, and the cultures were then analyzed at 21 DIV. Infection of neurons with CSPα lentiviruses resulted in ~2 fold overexpression of CSPα and exogenous CSPα was correctly targeted to presynaptic termini (Fig. S3B). Importantly, overexpression of CSPα, but not the $CSP\alpha_{QPN}$ mutant, rescues the decrease in synapse numbers in the CSPα KO to wildtype levels (Fig. 4G), confirming that loss of Hsc70-CSPα chaperone activity is causal for the synapse loss seen in Fig. 4B and underscores that CSPα is a key synapse maintenance gene. Furthermore, CSPα overexpression in CSPα KO neurons increases the levels of SNAP-25 significantly, with dynamin 1 showing a similar trend (Fig. 4E–F). Together, our data show that CSPα is both necessary and sufficient for maintaining its client protein levels at the synapse.

CSPα Regulates the Oligomerization of Dynamin 1

Dynamin 1 has five domains comprising an N-terminal GTPase domain, the bundle signaling element, the stalk, a pleckstrin homology (PH) domain and a C-terminal proline rich domain (PRD) (Fig. S4A). The crystal structure of human dynamin 1 was recently published, revealing that the basic functional unit of dynamin 1 is a dimer in which the stalk domains are arranged in a criss-cross fashion (Faelber et al, 2011; Ford et al., 2011). Dynamin 1 oligomerizes by addition of dimers to form a ring around the neck of clathrin coated pits, such that the GTPase domains in adjacent rings interact, enabling GTP-dependent fission. Via its PRD domain, dynamin 1 recruits other components of the endocytic machinery such as endophilins and amphiphysins (Ramachandran et al., 2007; Slepnev et al., 1998).

Dynamin 1 undergoes a series of conformational changes and protein interactions to execute its endocytic function. We wanted to know which of these steps may be regulated by CSPα. In order to capture native dynamin 1 assemblies, we chose to crosslink dynamin 1 *in situ* in intact synaptosomes using the membrane permeable, non-cleavable crosslinker, DSS. As seen in Fig 5A, dynamin 1 exists primarily as higher-order oligomers (dynamin $1_{n>6}$), tetramers, and monomers in wildtype synaptosomes. In contrast, CSPα KO synaptosomes have fewer dynamin 1 oligomers and tetramers (Fig. 5A–B). Significantly, this effect is selective for higher-order dynamin 1 species with no change in monomer levels, such that

the dynamin oligomer/monomer ratio is reduced by 40% (Fig. 5C), indicating a defect in dynamin 1 oligomerization. To discern if this effect is due to a decrease in dynamin 1 levels, we carried out similar experiments on dynamin 1 heterozygous mice which have 50% less dynamin 1 than wild-types (Ferguson et al., 2007), similar to CSPα KO mice. Intriguingly, in dynamin 1 heterozygotes we observed a uniform decrease in all dynamin 1 species including the monomer (Fig. 5D–E), so the dynamin oligomer/monomer ratio was unchanged (Fig. 5F). This is in line with the fact that dynamin 1 heterozygotes are phenotypically normal and have no synaptic vesicle endocytic deficits (Ferguson et al., 2007). These *in vivo* crosslinking data demonstrate that in CSPα KO synapses, dynamin 1 self-assembly is impaired and this does not arise from lowered dynamin 1 levels.

We also examined the profile of higher-order dynamin 1 species in synaptosomes of wildtype and CSPα KO mice by non-reducing SDS-PAGE gels. We obtained similar results, with the CSPα KO showing lowered dynamin 1 oligomer levels (Fig. S4C–D). Together, these data strongly suggest that oligomerization of dynamin 1 is disrupted in CSPα KO synapses.

We next reconstituted CSPα-dependent oligomerization of dynamin 1 *in vitro*. Brain purified dynamin 1 was incubated with ATP alone or ATP, CSPα, and Hsc70 (Fig. 6A). The mixtures were then separated on SDS-PAGE gels and immunoblotted for dynamin 1. Notably, CSPα and Hsc70 together promote the oligomerization of dynamin 1, while CSPα alone or Hsc70 alone had no effect (Fig. 6B–C; S4E–F). Similar results were obtained with crosslinking (Fig. S4G–H). To obtain more accurate size information about the dynamin 1 oligomers, we separated these mixtures by gel chromatography on a Superose 6 column (Fig. 6D). Consistent with published literature, dynamin 1 alone largely runs as tetramer (~400 KDa) in these chromatograms (Faelber et al., 2011). Significantly, in the presence of the Hsc70-CSPα complex, the apparent molecular weight of dynamin 1 increases by ~200 KDa. Based on crystal structure, this would be consistent with addition of a dimer to the tetramer generating a hexamer. As would be expected of a chaperone, CSPα is not bound to hexameric dynamin 1 (see lanes 7–13 in Fig 6D). Further, we showed that CSPα binds N-terminal regions in dynamin 1 that are important for self-assembly (Fig. S4B). Collectively these data demonstrate that CSPα functions to catalyze the dynamin 1 polymerization step in synaptic vesicle endocytosis.

Dual Mode of CSPα Action

Our identification of two key players in the synaptic vesicle cycle -SNAP-25 and Dynamin 1- as clients for the CSPα-Hsc70 chaperone complex, called for a closer examination of their interactions and functional consequences. The two proteins have distinct structures. SNAP-25 is a natively unfolded protein that acquires a coiled-coiled structure when it forms a SNARE complex (Fasshauer et al., 1997), while dynamin 1 has a folded rod-like structure with exposed hydrophobic patches that participate in oligomerization (Faelber et al., 2011; Ford et al., 2011). We have shown SNAP-25 is recruited to this complex via Hsc70 binding, while dynamin 1 binds via CSPα (Fig. 3D). Hsc70 typically binds exposed unfolded, hydrophobic sequences such as in monomeric SNAP-25. The CSPα-Hsc70-SNAP-25 interaction may then serve to promote protein-protein interactions such as SNARE complex assembly or protect unfolded SNAP-25 from degradation. To distinguish between these options, we measured SNARE complex and monomeric SNAP-25 levels in wildtype and CSPα KO synaptosomes. What we observe is a uniform decrease in both SNARE complexes and monomeric SNAP-25, such that their ratio is unchanged (Fig. S5A–C), similar to heterozygous SNAP-25 KO mice (Washbourne et al., 2002). This suggests that the CSPα-Hsc70 complex, as proposed recently, is probably protecting monomeric SNAP-25 from misfolding and degradation (Sharma et al., 2011). Indeed, we find increased ubiquitination of SNAP-25 in CSPα KO synapses by immunoprecipitations (Fig S5E–F). We also find that

SNAP-25 aggregation is not increased in these brains (Fig. S5D). These results indicate that in the CSPα KO, there is less available SNAP-25 for SNARE complex assembly, resulting in a partial loss-of-SNAP-25 function.

In the case of dynamin 1, the CSPα KO shows a dramatic redistribution of the oligomeric pattern of dynamin 1 (Fig. 5A–C) that was not observed in the dynamin 1 heterozygotes (Fig. 5D–F). This would argue that CSPα-Hsc70 complex directly participates in oligomerization of dynamin 1 by switching its conformation to one that facilitates self-assembly. It also suggests that CSPα is probably not functioning to protect dynamin 1 from degradation and in fact, we do not find that dynamin 1 is ubiquitinated (data not shown). The apparent decrease in dynamin 1 levels in CSPα KO synapses may be accounted for by a selective loss of dynamin 1 from the membrane synaptic fractions (Fig. S2A–B), again consistent with a deficit in membrane-associated oligomerization. We also ruled out that dynamin 1 is aggregated in the CSPα KO (Fig. S5D).

To investigate whether deletion of CSPα leads to a partial loss-of-dynamin 1 function, we explored if the CSPα KO phenocopies any aspects of the dynamin 1 KO. Similar to the CSPα KO, deletion of dynamin 1 in mice leads to activity-dependent synaptic dysfunction and perinatal lethality after 2 weeks. At an ultrastructural level, CSPα KO synapses have fewer synaptic vesicles (Fig. 5G–H) like the dynamin 1 KO (Ferguson et al., 2007; Hayashi et al., 2008). A decrement in synaptic vesicle number is found in many other endocytic mutants (Dickman et al., 2005) and is consistent with the hypothesis that the CSPα KO has endocytic deficits. In an accompanying paper submission, Rozas and colleagues have directly measured synaptic vesicle recycling in CSPα KO motor neurons using electrophysiology and synaptophysin pHluorin imaging and show deficits in dynamin-dependent synaptic vesicle endocytosis, consistent with a loss-of-dynamin 1 function in the CSPα KO. The distinct interactions of the Hsc70-CSPα chaperone complex with SNAP-25 and dynamin 1 reveal that this chaperone has a dual mode of action and is a testament to the versatility of this chaperone complex.

CSPα May Play a Role in Synapse Loss in Neurodegenerative Diseases

Synapse loss is a cardinal feature of neurodegenerative diseases such as Alzheimer's disease (Selkoe, 2002). Therefore, it was intriguing to determine if a decrement of CSPα-dependent synapse maintenance mechanism plays a role in neurodegenerative diseases. Such an involvement was hinted at by the interaction of CSPα with huntingtin (Miller et al., 2003) (Fig. 1D). Hence, we tested the levels of CSPα and Hsc70 in age-matched human control and Alzheimer's disease brains. Interestingly, protein levels of CSPα and Hsc70 were both decreased by approximately 40% in the frontal cortex of AD brains (Fig. S6), suggesting a possible role in synaptic degeneration. Consistent with previously published results, synaptophysin levels were also decreased in AD brains compared to age matched controls, and served as a positive control in this cohort (Masliah et al., 2001).

DISCUSSION

In this study, we sought to understand presynaptic mechanisms of synapse maintenance. Here we present the results of a comprehensive, unbiased proteomic screen designed to identify CSPα clients. We screened over 1500 unique synaptic proteins, using DIGE and iTRAQ with rigorous selection criteria and identified a set of 37 proteins whose levels were selectively decreased in CSPα KO synaptic fractions (Fig. 1; Table I). We experimentally verified the levels of 22 of these proteins by MRM or quantitative blotting (Table S2; Fig. 2A–D). This set of proteins comprises components of the Hsc70 chaperone network, as well as select exocytic, endocytic, signaling and cytoskeletal proteins. Due to the stringent criteria of this screen, we cannot rule out that we may have missed proteins showing modest

decreases and/or low abundance clients of CSPα. Notwithstanding this caveat, it is likely that the proteins we identified represent the majority of the CSPα interactome in the brain (Table I). Through a secondary screen on interactome members for CSPα binding, we identified SNAP-25 and dynamin 1 as clients of the CSPα chaperone complex (Fig. 3). Using a CSPα KO culture system, we could demonstrate that CSPα functions cell autonomously to maintain synapses and regulates both SNAP-25 and dynamin 1 protein levels (Fig. 4). It remains to be determined whether other high confidence interactome members such as Septin 3 and ARF-GEP are direct clients of CSPα.

The identification of dynamin 1 as a direct client of the CSPα/Hsc70 chaperone complex was intriguing as it broadened the envisioned role of CSPα in the nerve terminal. We therefore characterized the interaction between dynamin 1 and CSPα further. First, we showed that purified dynamin 1 accelerates the ATPase activity of the reconstituted CSPα/Hsc70 complex (Fig. 3F), confirming that it is a bona fide client. Next, we used multiple *in vivo* and *in vitro* approaches to demonstrate that (i) oligomerization of dynamin 1 is impaired in CSPα KO synapses (Fig. 5A–C) and (ii) Hsc70-CSPα can catalyze the oligomerization of dynamin 1 (Fig. 6, S4). Our data strongly suggest that CSPα promotes a conformational switch in dynamin 1 that facilitates its polymerization. This is in line with the other presynaptic Hsp40 co-chaperone auxilin, which acts to disassemble clathrin cages (Fotin et al., 2004). CSPα is the first protein known to promote the oligomerization of dynamin 1.

The identification of SNAP-25 and dynamin 1 as CSPα clients suggests that CSPα allows for efficient exo-endocytic coupling (Fig. 7). Several lines of evidence indicate that CSPα is well positioned to participate in exo-endocytic coupling. 1) The CSPα KO shows both exo- and endocytic deficits (Fernandez-Chacon, personal communication). Fernandez-Chacon and colleagues used synaptophysin-pHlourin to directly measure the kinetics of synaptic vesicle endocytosis at the neuromuscular junction of CSPα KO and find deficits in kinetics as well as recycling pool size that appear to be a consequence of impaired dynamin-dependent synaptic vesicle fission. Significantly, the biggest deficit in the CSPα KO appears to be endocytosis that occurs during stimulation. 2) CSPα being a synaptic vesicle protein, is most likely to act on SNAP-25 and dynamin 1 when the vesicle is in close proximity to the membrane, i.e. during exocytosis and endocytosis. Consistent with this, the largest changes in protein levels were observed in the membrane fractions (Table S2; Fig. S2A–B). 3) Since CSPα is likely to interact with dynamin 1 post vesicle fusion, CSPα may serve as a coincidence detector to accelerate the polymerization of dynamin 1 at only this juncture and facilitate synaptic vesicle endocytosis (Fig. 7). Interestingly, our study highlights that several steps of the synaptic vesicle cycle are being regulated by chaperones-- exo-endocytic coupling by CSPα, SNARE disassembly by NSF (Otto et al., 1997), and uncoating by auxillin (Fotin et al., 2004).

The most striking phenotype in the CSPα KO is the activity-dependent loss of synapses and neurodegeneration (Chandra et al., 2005; Garcia-Junco-Clemente et al., 2010; Schmitz et al., 2006). How the loss of chaperone activity of CSPα leads to disassembly of synaptic structures and neurodegeneration is an important and challenging question. Our identification of CSPα clients is the first step to addressing this question. Of particular interest is how actin binding properties of dynamin 1 (Orth et al., 2003; Schafer, 2002) and the Hsc70 binding protein BASP1 (Fig. 3A) participate in synapse structural stability. The relationship between synapse stability and neurodegeneration in the CSPα KO is fascinating, especially in light of our findings of selective decreases in the levels of CSPα and Hsc70 in postmortem Alzheimer's disease frontal cortex compared to age matched controls (Fig. S6). The recent identification of CSPα as a human neurodegenerative disease gene (Nosková et al., 2011) further emphasizes the importance of synapse maintenance to neurodegenerative

diseases. Hence, investigating the CSPα-dependent synapse maintenance mechanism further may identify novel and early therapeutic targets for treating neurodegenerative diseases.

In summary, we have provided mechanistic insight into CSPα function at the presynaptic terminal. We show that CSPα acts on SNAP-25 and dynamin 1, and allows for maintenance of synaptic function and structure.

EXPERIMENTAL PROCEDURES

A detailed description of the experimental procedures used is available online in the Supplement.

Mice

Generation and characterization of CSPα KO mice have been previously published (Fernandez-Chacon et al., 2004). All mice were kept in accordance with an IACUC approved animal protocol. Heterozygous dynamin 1 brains were kindly provided by Pietro De Camilli, Yale University.

Human Samples

Frozen brains from Alzheimer patients (Braak stage V–VI) and age-matched controls (n=9/group) were used in this study. The brain region analyzed was frontal cortex Brodmann Area 9 (BA9). Brains were accessed and employed under the auspices of IRB and IACUC guidelines administrated by the Nathan Kline Institute/New York University Langone Medical Center.

Synaptosome Fractionation

Wildtype and CSPα KO mice were fractionated according to the protocol of (Huttner et al., 1983). Briefly, freshly dissected brains were homogenized in isotonic sucrose to prepare synaptosomes. The synaptosomes were hypotonically lyzed and further fractionated into synaptic cytosol, membrane and vesicle fractions.

Mass Spectrometry

A quantitative analysis of the synaptic proteome of wildtype and CSPα mice was performed using DIGE according to previously published protocols (Wu, 2006). Equal amounts of protein from wildtype and CSPα samples were differentially labeled *in vitro* with Cy3 and Cy5 N-hydroxysuccinimidyl ester dyes and separated on two-dimensional gels. Differentially expressed protein spots were robotically excised and subjected to in-gel trypsinization. The peptides were analyzed on a matrix-assisted laser desorption/ionization time-of-flight spectrometer (MALDI ToF/ToF; Applied Biosystems model 4800). The resulting, uninterpreted MS/MS spectra were searched against the IPI mouse database 3.27 using Mascot algorithms to enable high-throughput protein identification.

Wildtype and CSPα KO samples were subjected to 4-plex iTRAQ with technical replicates as described (Davalos et al., 2010). The samples were trypsin digested, labeled with iTRAQ tags, pooled, fractionated by cation exchange and the individual peptides were run on an Applied Biosystems API Q-Star XL mass spectrometer. iTRAQ quantitation and protein identification were performed using the Paragon search algorithm (Shilov et al., 2007) in ProteinPilot 2.0 software against the IPI mouse database.

Stringent criteria were used to identify potential CSPα clients. For the iTRAQ experiments, at least 2 independent peptides with valid iTRAQ reporter ion ratios, exhibiting a minimum of two iTRAQ reporter ions with a summed S/N ratio >9 were required to be included in the

analysis. A cutoff was set at 0.7 for down-regulated proteins and 1.4 for up-regulated proteins or $p<0.01$ whichever was more stringent was used for both DIGE and iTRAQ experiments. Principal Components Analysis was used to examine the consistency of the technical replicates and DIGE experiments and proteins showing inconsistencies were disregarded.

Proteins that showed statistically significant changes by DIGE and iTRAQ were selected for protein-level quantification using Multiple Reaction Monitoring methods. All analyses were carried out on a 5500 Q-TRAP instrument coupled to an online Waters nanoACQUITY Ultra High Pressure Liquid Chromatography system. Data were initially processed using MRMPilot 2.0, Analyst 1.5 with MIDAS, and Multiquant 2.0 software. Peptide identification was confirmed using MASCOT 2.3. All raw mass spectrometry data are deposited in the Yale Protein Expression Database (YPED) (Shifman et al., 2007) and are publically available through http://yped.med.yale.edu/repository. Access Code: cqVUPu

Quantification immunoblotting

Synaptosomal proteins, hippocampal neuronal culture extracts or human tissue homogenates were subject to SDS-PAGE and western blotting. The proteins levels were quantified using conjugated IRDye secondary antibodies on a Li-COR Odyssey infrared imaging system. Actin and tubulin were used as internal controls.

ATPase Assay

ATPase activity was assayed using colormetric approach as described (Chamberlain and Burgoyne, 1997a). Briefly, 1 μmol each of purified protein was incubated in ATPase assay buffer (10 mM $MgCl_2$, 5 mM KCl, 50 mM Tris, pH 7.5) for 5 minutes, followed by addition of 1 mM ATP to start the reaction. The free phosphate released was determined every 4 minutes using malachite green and measuring the absorbance at 650 nm.

Image Analysis of Neurons

Hippocampal neuron cultures were immunostained using synaptophysin as presynaptic marker and MAP2 as a dendritic marker. Regions of interest were selected for each image such that areas with coalescing dendrites were excluded. Volocity 5.4.1 software was used to quantify all the presynaptic puncta within 5 iterations of the dendrite fluorescence using a custom script.

In vitro Polymerization

1 or 2 μM dynamin 1 was incubated with equimolar CSPα or Hsc70 in the presence of 1 mM ATP at 37°C. The incubation mixtures were first sep arated on a Superose 6 column or directly analyzed on SDS-PAGE gels and immunoblotted for dynamin 1.

Crosslinking of Synaptosomes

Synaptosomes were preincubated for 15 minutes at 37°C and then incubated for 1 minute at room temperature after adding 1 mM Disuccinimidyl suberate (DSS). The reaction was stopped by adding 100 mM Tris-HCl, pH 8.0 for 15 minutes at room temperature.

Statistics

All values are presented as the mean ± SEM, and $p< 0.05$ was considered statistically significant. Calculations were performed using the Graph Prism 4 software (San Diego, CA)

HIGHLIGHTS

- CSPα is required for synapse maintenance
- Quantitative proteomics identified 22 putative CSPα clients
- CSPα chaperones SNAP-25 and dynamin 1, coupling exocytosis and endocytosis
- CSPα promotes dynamin 1 oligomerization

Supplementary Material

Refer to Web version on PubMed Central for supplementary material.

Acknowledgments

We would like to thank Thomas Südhof, Pietro De Camilli, Art Horwich, Thomas Biederer, and members of our laboratory for critical discussions related to this paper. We would like to thank Karina Vargas for technical help with electron microscopy and Becket Greten-Harrison for quantitative immunoblotting of human brain samples. This work was supported by the YCCI Scholar Award (CTSA grant UL1 RR024139; SSC), R01NS064963 (SSC), an Anonymous Foundation (SSC), W.M. Keck Foundation grant (SSC), NIDA Neuroproteomic Pilot Grant (5 P30 DA018343-07; SSC), Anderson Fellowship (YQZ), NSF Graduate Research Fellowship (MH) and AG14449 (SDG).

REFERENCES

Boal F, Laguerre M, Milochau A, Lang J, Scotti PA. A charged prominence in the linker domain of the cysteine-string protein Cspalpha mediates its regulated interaction with the calcium sensor synaptotagmin 9 during exocytosis. FASEB J. 2011; 25:132–143. [PubMed: 20847230]

Braun JE, Wilbanks SM, Scheller RH. The cysteine string secretory vesicle protein activates Hsc70 ATPase. J Biol Chem. 1996; 271:25989–25993. [PubMed: 8824236]

Chamberlain LH, Burgoyne RD. Activation of the ATPase activity of heat-shock proteins Hsc70/Hsp70 by cysteine-string protein. Biochem J. 1997a; 322(Pt 3):853–858. [PubMed: 9148760]

Chamberlain LH, Burgoyne RD. The molecular chaperone function of the secretory vesicle cysteine string proteins. J Biol Chem. 1997b; 272:31420–31426. [PubMed: 9395474]

Chandra S, Gallardo G, Fernandez-Chacon R, Schluter OM, Sudhof TC. Alpha-synuclein cooperates with CSPalpha in preventing neurodegeneration. Cell. 2005; 123:383–396. [PubMed: 16269331]

Davalos A, Fernandez-Hernando C, Sowa G, Derakhshan B, Lin MI, Lee JY, Zhao H, Luo R, Colangelo C, Sessa WC. Quantitative proteomics of caveolin-1-regulated proteins: characterization of polymerase i and transcript release factor/CAVIN-1 IN endothelial cells. Mol Cell Proteomics. 2010; 9:2109–2124. [PubMed: 20585024]

DeLuca-Flaherty C, McKay DB, Parham P, Hill BL. Uncoating protein (hsc70) binds a conformationally labile domain of clathrin light chain LCa to stimulate ATP hydrolysis. Cell. 1990; 62:875–887. [PubMed: 1975516]

Dickman DK, Horne JA, Meinertzhagen IA, Schwarz TL. A slowed classical pathway rather than kiss-and-run mediates endocytosis at synapses lacking synaptojanin and endophilin. Cell. 2005; 123:521–533. [PubMed: 16269341]

Evans GJ, Morgan A, Burgoyne RD. Tying everything together: the multiple roles of cysteine string protein (CSP) in regulated exocytosis. Traffic. 2003; 4:653–659. [PubMed: 12956868]

Faelber K, Posor Y, Gao S, Held M, Roske Y, Schulze D, Haucke V, Noé F, Daumke O. Crystal structure of nucleo-tide free dynamin. Nature. 2011; 477:556–560. [PubMed: 21927000]

Fasshauer D, Otto H, Eliason WK, Jahn R, Brünger AT. Structural changes are associated with soluble N-ethylmaleimide-sensitive fusion protein attachment protein receptor complex formation. J Biol Chem. 1997; 272:28036–28041. [PubMed: 9346956]

Ferguson SM, Brasnjo G, Hayashi M, Wolfel M, Collesi C, Giovedi S, Raimondi A, Gong LW, Ariel P, Paradise S, et al. A selective activity-dependent requirement for dynamin 1 in synaptic vesicle endocytosis. Science. 2007; 316:570–574. [PubMed: 17463283]

Fernandez-Chacon R, Wolfel M, Nishimune H, Tabares L, Schmitz F, Castellano-Munoz M, Rosenmund C, Montesinos ML, Sanes JR, Schneggenburger R, et al. The synaptic vesicle protein CSP alpha prevents presynaptic degeneration. Neuron. 2004; 42:237–251. [PubMed: 15091340]

Ford MG, Jenni S, Nunnari J. The crystal structure of dynamin. Nature. 2011; 477:561–566. [PubMed: 21927001]

Fotin A, Cheng Y, Grigorieff N, Walz T, Harrison SC, Kirchhausen T. Structure of an auxilin-bound clathrin coat and its implications for the mechanism of uncoating. Nature. 2004; 432:649–653. [PubMed: 15502813]

Fujimoto M, Nakai A. The heat shock factor family and adaptation to proteotoxic stress. FEBS J. 2010; 277:4112–4125. [PubMed: 20945528]

Garcia-Junco-Clemente P, Cantero G, Gomez-Sanchez L, Linares-Clemente P, Martinez-Lopez JA, Lujan R, Fernandez-Chacon R. Cysteine string protein-alpha prevents activity-dependent degeneration in GABAergic synapses. J Neurosci. 2010; 30:7377–7391. [PubMed: 20505105]

Greaves J, Chamberlain LH. Dual role of the cysteine-string domain in membrane binding and palmitoylation-dependent sorting of the molecular chaperone cysteine-string protein. Mol Biol Cell. 2006; 17:4748–4759. [PubMed: 16943324]

Grutzendler J, Gan WB. Two-photon imaging of synaptic plasticity and pathology in the living mouse brain. NeuroRx. 2006; 3:489–496. [PubMed: 17012063]

Gundersen CB, Umbach JA. Suppression cloning of the cDNA for a candidate subunit of a presynaptic calcium channel. Neuron. 1992; 9:527–537. [PubMed: 1326297]

Hayashi M, Raimondi A, O'Toole E, Paradise S, Collesi C, Cremona O, Ferguson SM, De Camilli P. Cell- and stimulus-dependent heterogeneity of synaptic vesicle endocytic recycling mechanisms revealed by studies of dynamin 1-null neurons. Proc Natl Acad Sci U S A. 2008; 105:2175–2180. [PubMed: 18250322]

Holtmaat A, Svoboda K. Experience-dependent structural synaptic plasticity in the mammalian brain. Nat Rev Neurosci. 2009; 10:647–658. [PubMed: 19693029]

Holtmaat A, Wilbrecht L, Knott GW, Welker E, Svoboda K. Experience-dependent and cell-type-specific spine growth in the neocortex. Nature. 2006; 441:979–983. [PubMed: 16791195]

Huttner WB, Schiebler W, Greengard P, De Camilli P. Synapsin I (protein I), a nerve terminal-specific phosphoprotein. III. Its association with synaptic vesicles studied in a highly purified synaptic vesicle preparation. J Cell Biol. 1983; 96:1374–1388. [PubMed: 6404912]

Johnson JN, Ahrendt E, Braun JE. CSPalpha: the neuroprotective J protein. Biochem Cell Biol. 2010; 88:157–165. [PubMed: 20453918]

Kampinga HH, Craig EA. The HSP70 chaperone machinery: J proteins as drivers of functional specificity. Nat Rev Mol Cell Biol. 2010; 11:579–592. [PubMed: 20651708]

Leveque C, Pupier S, Marqueze B, Geslin L, Kataoka M, Takahashi M, De Waard M, Seagar M. Interaction of cysteine string proteins with the alpha1A subunit of the P/Q-type calcium channel. J Biol Chem. 1998; 273:13488–13492. [PubMed: 9593683]

Lin YC, Koleske AJ. Mechanisms of synapse and dendrite maintenance and their disruption in psychiatric and neurodegenerative disorders. Annu Rev Neurosci. 2010; 33:349–378. [PubMed: 20367247]

Magga JM, Jarvis SE, Arnot MI, Zamponi GW, Braun JE. Cysteine string protein regulates G protein modulation of N-type calcium channels. Neuron. 2000; 28:195–204. [PubMed: 11086994]

Masliah E, Mallory M, Alford M, DeTeresa R, Hansen LA, McKeel DW Jr, Morris JC. Altered expression of synaptic proteins occurs early during progression of Alzheimer's disease. Neurology. 2001; 56:127–129. [PubMed: 11148253]

Miller LC, Swayne LA, Chen L, Feng ZP, Wacker JL, Muchowski PJ, Zamponi GW, Braun JE. Cysteine string protein (CSP) inhibition of N-type calcium channels is blocked by mutant huntingtin. J Biol Chem. 2003; 278:53072–53081. [PubMed: 14570907]

Natochin M, Campbell TN, Barren B, Miller LC, Hameed S, Artemyev NO, Braun JE. Characterization of the G alpha(s) regulator cysteine string protein. J Biol Chem. 2005; 280:30236–30241. [PubMed: 15972823]

Nie Z, Ranjan R, Wenniger JJ, Hong SN, Bronk P, Zinsmaier KE. Overexpression of cysteine-string proteins in Drosophila reveals interactions with syntaxin. J Neurosci. 1999; 19:10270–10279. [PubMed: 10575024]

Nikolaus S, Antke C, Muller HW. In vivo imaging of synaptic function in the central nervous system: I. Movement disorders and dementia. Behav Brain Res. 2009; 204:1–31. [PubMed: 19523490]

Nosková L, Stránecký V, Hartmannová H, Přistoupilová A, Barešová V, Ivánek R, Hůlková H, Jahnová H, van der Zee J, Staropoli JF, et al. Mutations in DNAJC5, encoding cysteine-string protein alpha, cause autosomal-dominant adult-onset neuronal ceroid lipofuscinosis. Am J Hum Genet. 2011; 89:241–252. [PubMed: 21820099]

Ohyama T, Verstreken P, Ly CV, Rosenmund T, Rajan A, Tien AC, Haueter C, Schulze KL, Bellen HJ. Huntingtin-interacting protein 14, a palmitoyl transferase required for exocytosis and targeting of CSP to synaptic vesicles. J Cell Biol. 2007; 179:1481–1496. [PubMed: 18158335]

Orth JD, McNiven MA. Dynamin at the actin-membrane interface. Curr Opin Cell Biol. 2003; 15:31–39. [PubMed: 12517701]

Otto H, Hanson PI, Jahn R. Assembly and disassembly of a ternary complex of synaptobrevin, syntaxin, and SNAP-25 in the membrane of synaptic vesicles. Proc Natl Acad Sci U S A. 1997; 94:6197–6201. [PubMed: 9177194]

Ramachandran R, Surka M, Chappie JS, Fowler DM, Foss TR, Song BD, Schmid SL. The dynamin middle domain is critical for tetramerization and higher-order self-assembly. EMBO J. 2007; 26:559–566. [PubMed: 17170701]

Sahi C, Craig EA. Network of general and specialty J protein chaperones of the yeast cytosol. Proc Natl Acad Sci U S A. 2007; 104:7163–7168. [PubMed: 17438278]

Sakisaka T, Meerlo T, Matteson J, Plutner H, Balch WE. Rab-alphaGDI activity is regulated by a Hsp90 chaperone complex. EMBO J. 2002; 21:6125–6135. [PubMed: 12426384]

Schafer DA. Coupling actin dynamics and membrane dynamics during endocytosis. Curr Opin Cell Biol. 2002; 14:76–81. [PubMed: 11792548]

Schmitz F, Tabares L, Khimich D, Strenzke N, de la Villa-Polo P, Castellano-Munoz M, Bulankina A, Moser T, Fernandez-Chacon R, Sudhof TC. CSPalpha-deficiency causes massive and rapid photoreceptor degeneration. Proc Natl Acad Sci U S A. 2006; 103:2926–2931. [PubMed: 16477021]

Selkoe DJ. Alzheimer's disease is a synaptic failure. Science. 2002; 298:789–791. [PubMed: 12399581]

Sharma M, Burre J, Sudhof TC. CSPalpha promotes SNARE-complex assembly by chaperoning SNAP-25 during synaptic activity. Nat Cell Biol. 2011; 13:30–39. [PubMed: 21151134]

Shifman MA, Li Y, Colangelo CM, Stone KL, Wu TL, Cheung KH, Miller PL, Williams KR. YPED: a web-accessible database system for protein expression analysis. J Proteome Res. 2007; 6:4019–4024. [PubMed: 17867667]

Shilov IV, Seymour SL, Patel AA, Loboda A, Tang WH, Keating SP, Hunter CL, Nuwaysir LM, Schaeffer DA. The Paragon Algorithm, a next generation search engine that uses sequence temperature values and feature probabilities to identify peptides from tandem mass spectra. Mol Cell Proteomics. 2007; 6:1638–1655. [PubMed: 17533153]

Slepnev VI, Ochoa GC, Butler MH, Grabs D, De Camilli P. Role of phosphorylation in regulation of the assembly of endocytic coat complexes. Science. 1998; 281:821–824. [PubMed: 9694653]

Tannu NS, Hemby SE. Methods for proteomics in neuroscience. Prog Brain Res. 2006; 158:41–82. [PubMed: 17027691]

Tobaben S, Thakur P, Fernandez-Chacon R, Sudhof TC, Rettig J, Stahl B. A trimeric protein complex functions as a synaptic chaperone machine. Neuron. 2001; 31:987–999. [PubMed: 11580898]

Umbach JA, Zinsmaier KE, Eberle KK, Buchner E, Benzer S, Gundersen CB. Presynaptic dysfunction in Drosophila csp mutants. Neuron. 1994; 13:899–907. [PubMed: 7946336]

Voisine C, Pedersen JS, Morimoto RI. Chaperone networks: tipping the balance in protein folding diseases. Neurobiol Dis. 2010; 40:12–20. [PubMed: 20472062]

Washbourne P, Thompson PM, Carta M, Costa ET, Mathews JR, Lopez-Bendito G, Molnar Z, Becher MW, Valenzuela CF, Partridge LD, et al. Genetic ablation of the t-SNARE SNAP-25 distinguishes mechanisms of neuroexocytosis. Nat Neurosci. 2002; 5:19–26. [PubMed: 11753414]

Wu TL. Two Dimensional Difference Gel Electrophoresis. New and Emerging Proteomics Techniques. 2006; 328:71–96.

Yocum AK, Chinnaiyan AM. Current affairs in quantitative targeted proteomics: multiple reaction monitoring-mass spectrometry. Brief Funct Genomic Proteomic. 2009; 8:145–157. [PubMed: 19279071]

Zinsmaier KE, Bronk P. Molecular chaperones and the regulation of neurotransmitter exocytosis. Biochem Pharmacol. 2001; 62:1–11. [PubMed: 11377391]

Zinsmaier KE, Eberle KK, Buchner E, Walter N, Benzer S. Paralysis and early death in cysteine string protein mutants of Drosophila. Science. 1994; 263:977–980. [PubMed: 8310297]

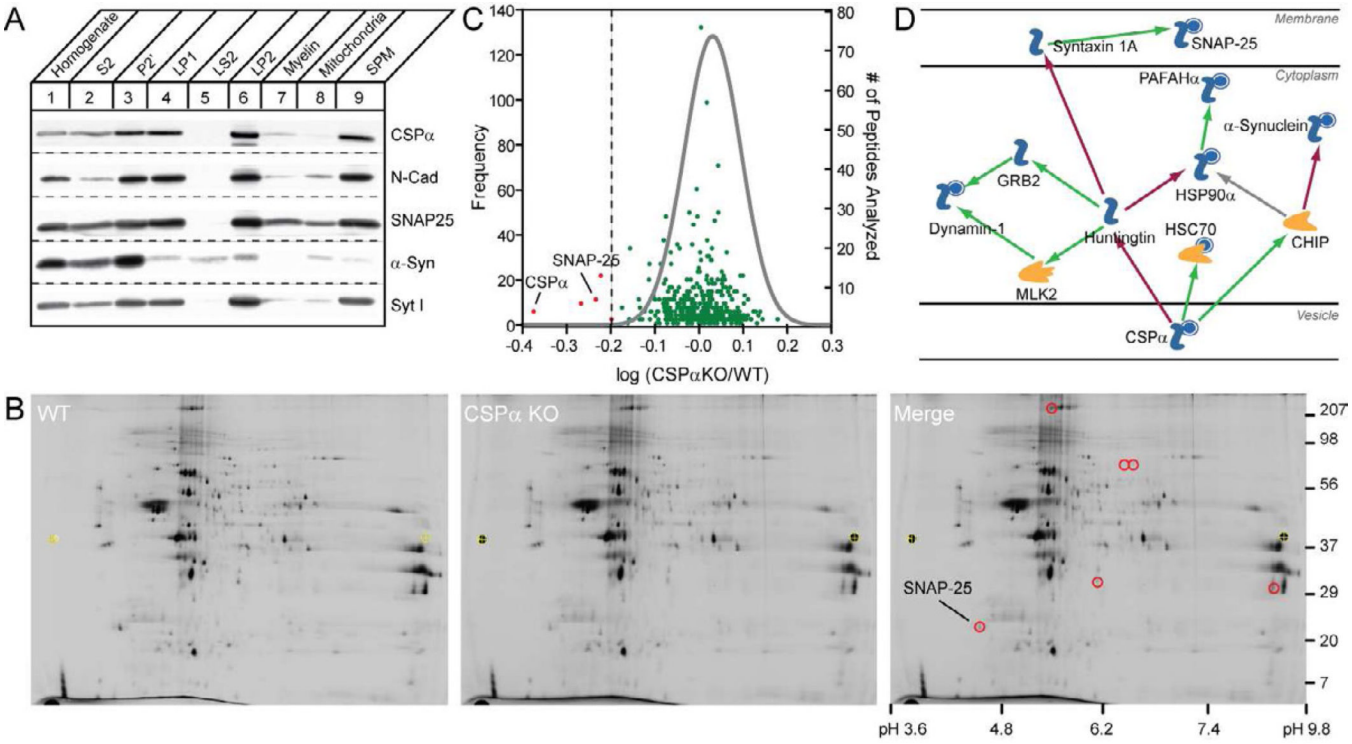

Figure 1. Quantitative proteomics reveals the repertoire of proteins exhibiting decreased levels in CSPα KO synapses

A. Subcellular fractionation of wildtype brains to obtain synaptic vesicle, plasma membrane and cytosolic fractions. Equal protein amounts (20 μg) were separated on SDS-PAGE gels and blotted for the denoted proteins. N-cadherin (N-Cad), synaptotagmin I (Syt I) and α-synuclein (α-Syn) were used as synaptic plasma membrane, vesicle and cytosolic fraction markers, respectively. **B.** DIGE gel of synaptic plasma membrane fractions. Wildtype (WT) samples were labeled with Cy3 and CSPα KO with Cy5, mixed in equal amounts separated on two-dimensional gels. The gels were scanned in Cy3 and Cy5 channels and the scans were overlaid (Merge). The protein spots that exhibit decreased Cy5 labeling were identified by mass spectrometry. Such spots are highlighted in red in the Merge and include the t-SNARE SNAP-25. A total of 13 DIGE experiments were performed and analyzed to quantitatively compare all synaptic fractions. **C.** Volcano plot of iTRAQ experiment on synaptic vesicle fraction. The frequency distribution of peptides showing differences between wildtype and CSPα KO samples are plotted against the number of peptides used to identify each protein. The dotted line indicates the threshold used to consider proteins as putative CSPα clients. The largest changes were observed for CSPα and SNAP-25 and are noted. A total of 3 iTRAQ experiments were conducted and we analyzed ~500 proteins/ iTRAQ experiment. For individual iTRAQ spectra see Fig. S1. **D.** Gene Ontology analysis of CSPα containing networks. The shortest pathway algorithm was used to link CSPα to other synaptic proteins with a maximum of 3 links. Proteins noted with a blue circle were identified in our proteomic screen. Green arrows indicate positive interactions and red inhibitory interactions.

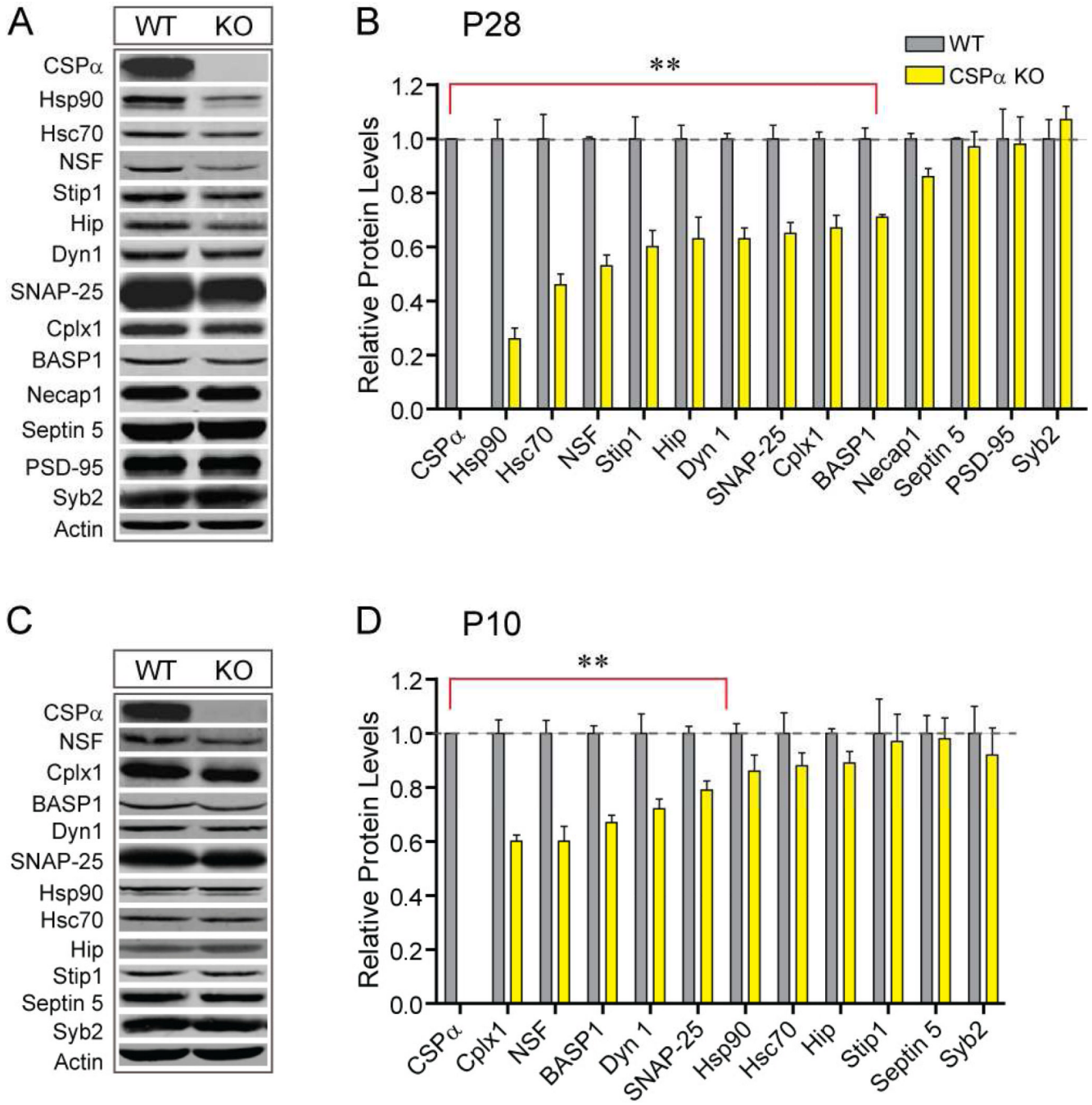

Figure 2. Validation of proteomic hits by quantitative immunoblotting

A–B. Synaptosomes were purified from P28 wildtype and CSPα KO mice (n=3/genotype). Equal amounts of protein (20 μg) were separated on SDS-PAGE gels and immunoblotted for the denoted proteins. The levels of individual proteins were determined by quantitative western blotting with IRDye conjugated secondary antibodies on a LI-COR infrared imaging system, using actin and tubulin as internal loading controls. **A.** Representative blots of proteins in wildtype and CSPα KO synaptosomes. **B.** The protein levels in CSPα KO relative to that of wildtype. Note the decreases in Dynamin 1, SNAP-25, Complexin I, BASP1 and NSF and select chaperone components in CSPα KO samples. For a similar analysis in P28 total brain homogenates see Fig. S2C. We confirmed that the observed

decreases occur post-transcriptionally for SNAP-25 and dynamin 1 (See Fig. S2D–E). **C–D.** Quantitative immunoblotting of P10 synaptosomes. Experiments were performed as described in A–B. The results show that decreases in the levels of dynamin 1, SNAP-25, complexin I, BASP1, and NSF precede synaptic degeneration. Abbreviations: Dyn 1, dynamin 1; Cplx1, Complexin I; Syb2, synaptobrevin 2. Mean ± S.E.M; **p<0.01.

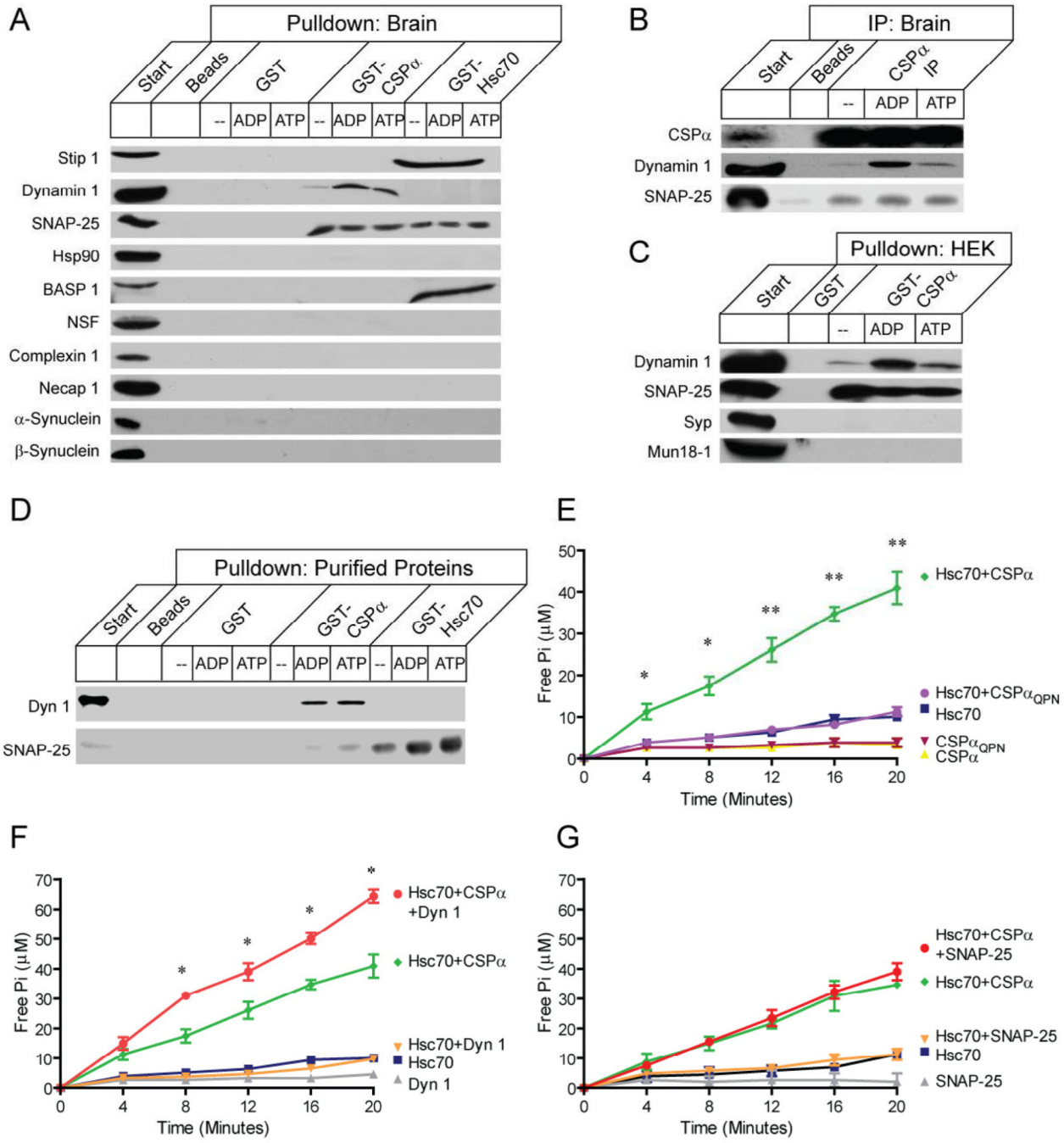

Figure 3. Interactions of putative clients with CSPα and Hsc70

A. Binding of putative clients to CSPα and Hsc70. Solubilized wildtype mouse brain homogenate (Start) was incubated with glutathione beads (lane 2), GST (lane 3–5), GST-CSPα (lane 6–8) or GST-Hsc70 (lanes 9–11) beads in the absence of nucleotides, or the presence of 5 mM ADP (lanes 4, 7, 10) or ATP (lanes 5, 8, 11), and bound proteins were analyzed by immunoblotting. The Hsc70 binding protein Stip1/HOP was used as a positive control. We identified that dynamin 1 binds CSPα and that SNAP-25 binds both CSPα and Hsc70 as shown previously (Sharma et al., 2011). **B.** CSPα was immunoprecipitated from brain homogenates and blotted for dynamin 1 and SNAP-25. Blots reveal that CSPα interacts with dynamin 1 and SNAP-25 *in vivo*. **C.** Binding of GST-CSPα to heterologously

expressed proteins. HEK 293T cells were transfected with expression constructs for the CSPα clients dynamin 1, SNAP-25, as well as controls synaptophysin (Syp) and Munc18-1. Detergent lysates from these cells was used to test binding to GST and GST-CSPα beads. **D.** Binding of GST-CSPα and GST-Hsc70 to purified dynamin 1 and SNAP-25 proteins. **E.** ATPase activity of Hsc70 in the presence of CSPα. Purified proteins were mixed as described and the ATP consumed was calculated using a Malachite green assay. The $CSP\alpha_{QPN}$ mutant was used as a negative control. **F–G.** Effect of protein clients on the ATPase activity of Hsc70. **F.** Dynamin 1 enhanced the ATPase activity of Hsc70 in the presence of CSPα, while SNAP-25 had a marginal effect (**G**). The data in all panels represents the average of at least 3 independent experiments (Mean ± S.E.M). * = $p < 0.05$, ** = $p < 0.01$.

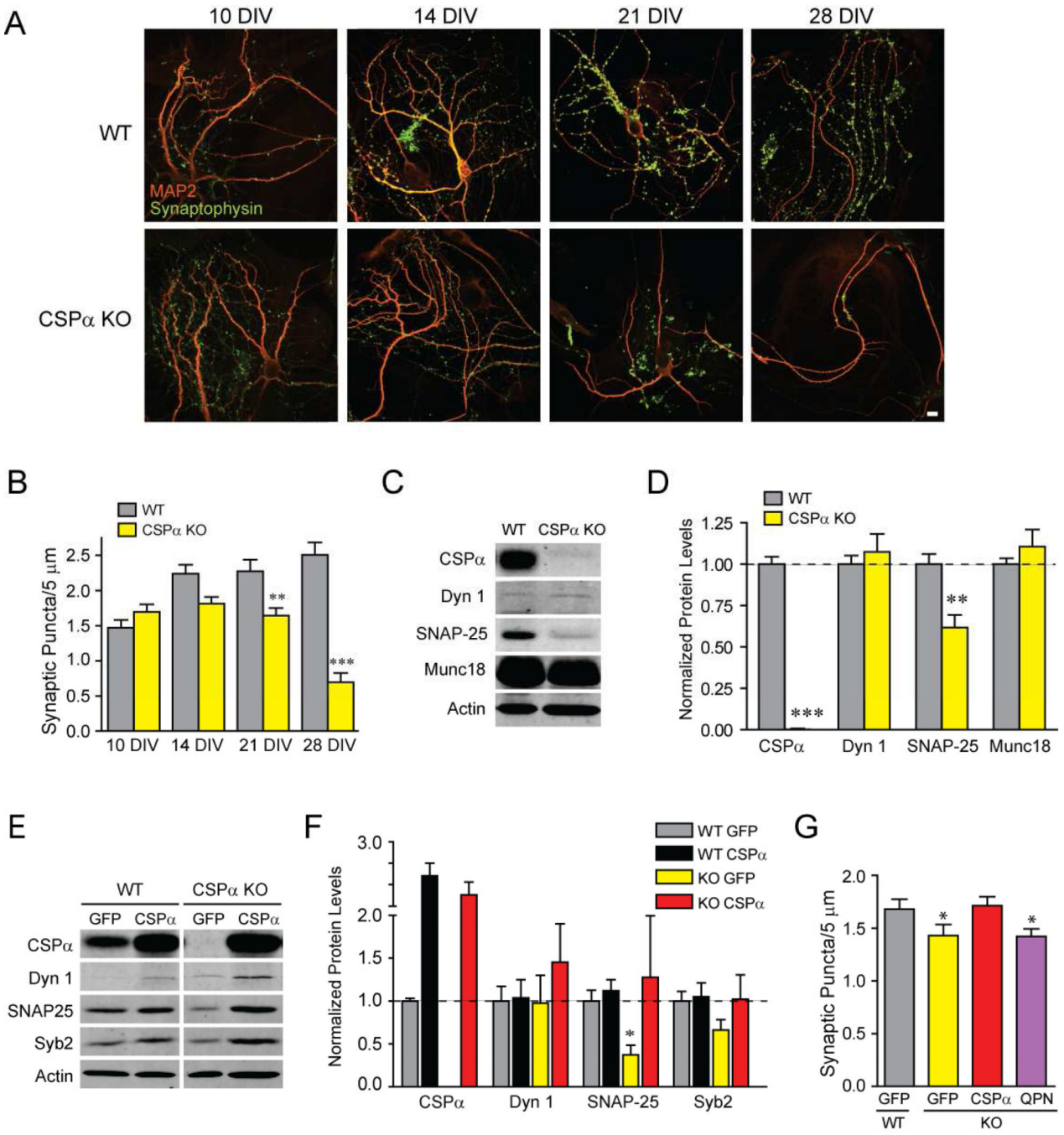

Figure 4. Analysis of CSPα clients in dissociated neuronal cultures

A. Wildtype and CSPα KO neurons in culture. Cultures of both genotypes were grown *in vitro* for the denoted days, fixed, and immunostained for dendritic marker MAP2 (red) and presynaptic marker synaptophysin (green). Representative images of wildtype and CSPα KO neurons are shown. Scale bar = 10 µm **B.** Quantitation of synapse density of wildtype and CSPα KO neurons as a function of days *in vitro* (DIV). Images similar to those shown in A. were quantified using a custom image script in Volocity. **C–D.** Quantification of CSPα client levels in cultured neurons. Wildtype and CSPα KO cultures (14 DIV; n=9 experiments) were detergent extracted and the lysates were subject to quantitative immunoblotting. **E–F.** Effect of lentiviral overexpression of CSPα on protein client levels.

First, we confirmed that that SNAP-25 and dynamin 1 are co-localized with CSPα and lentivirally expressed CSPα is targeted to presynaptic termini in these cultures (See Fig. S3). Then hippocampal neurons of the two genotypes were infected at 5 DIV and analyzed by quantitative immunoblotting at 21 DIV. We determined that CSPα can increase SNAP-25 and dynamin 1 levels. **G.** Effect of lentiviral overexpression of CSPα on synapse number. Hippocampal neurons of the two genotypes were infected at 5 DIV and analyzed by quantitative immunoblotting at 21 DIV. We determined that overexpression of CSPα in CSPα KO neurons can rescue synapse numbers to wildtype levels but the $CSP\alpha_{QPN}$ mutant does not. The data in all panels represents the average of at least 3 independent experiments (Mean ± S.E.M). * = $p < 0.05$, ** = $p < 0.01$.

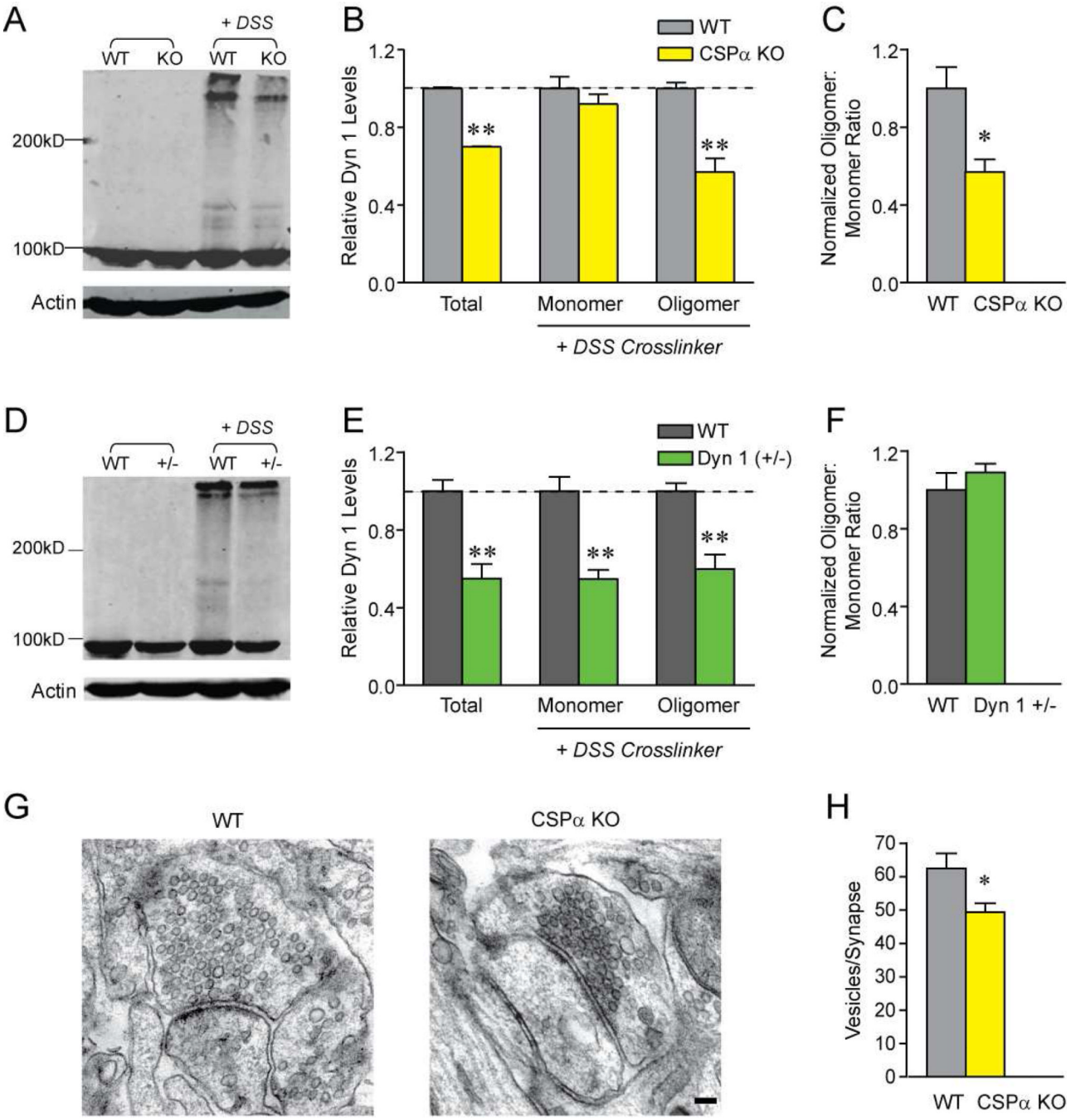

Figure 5. Characterization of the dynamin 1-CSPα interaction *in vivo*

A. Dynamin 1 oligomer profile in wildtype and CSPα KO synapses. Synaptosomes from wildtype (WT) and CSPα KO (KO) brains were treated without or with DSS, a membrane permeable, non-cleavable crosslinker (+DSS); the samples separated on SDS-PAGE gels under reducing conditions and blotted for dynamin 1. As seen in the gel, CSPα KO synaptosomes have a select decrease in oligomeric forms of dynamin 1. **B.** Quantification of dynamin 1 species in wildtype and CSPα KO synaptosomes after crosslinking (n=3 experiments). For synaptic dynamin 1 oligomer profile in the absence of crosslinking see Figure S4C–D. **C.** Quantification of the dynamin 1 oligomer/monomer ratio in wildtype and CSPα KO synaptosomes. **D.** Dynamin 1 oligomer profile in wildtype (WT) and dynamin 1

heterozygous (+/−) synaptosomes. Samples of the denoted genotypes were treated without or with DSS as described in A. **E.** Quantification of dynamin 1 species in wildtype and dynamin 1 heterozygous synaptosomes after crosslinking. **F.** Quantification of the dynamin 1 oligomer/monomer ratio in wildtype and dynamin 1 heterozygous synaptosomes. For a comparable analysis on SNAP-25, see Fig. S5A–C. **G–H.** Morhphometeric analysis of CSPα KO synapses. **G.** Representative WT and CSPα KO synapses in culture (scale bar = 250 nm). Note presence of fewer vesicles in CSPα KO synapse **H.** Synaptic vesicle number in wildtype and CSPα KO cultures (n=113 WT and 108 CSPα KO synapses). Mean ± S.E.M, * = $p < 0.05$, ** = $p < 0.01$.

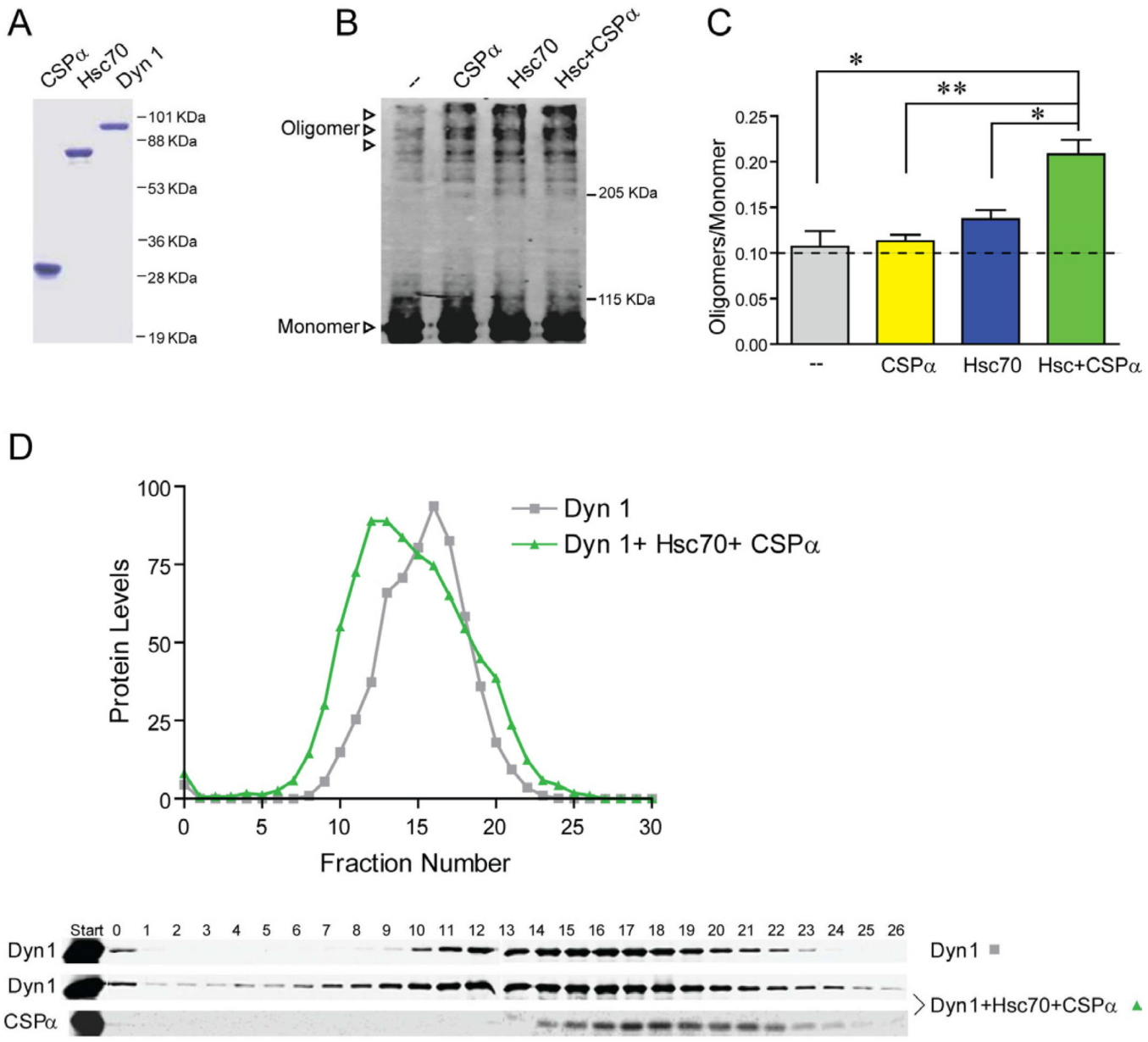

Figure 6. The CSPα chaperone complex promotes oligomerization of dynamin 1

A. Coomassie gel of brain purified dynamin 1 and recombinantly purified CSPα and Hsc70 (3 μg each). **B.** *In vitro* polymerization of dynamin 1. Purified dynamin 1 in buffer containing 1 mM DTT was mixed with the equimolar CSPα or Hsc70 and incubated for 1 hour at 37°C in the presence of 1 mM ATP. The mixtures were separated on non-reducing SDS-PAGE gels without boiling and western blotted for dynamin 1. For gels run under reducing conditions, see Fig S4E–F **C**. Quantification of dynamin 1 oligomers and monomers (n=3 experiments; Mean ± S.E.M). For *in vitro* crosslinking results see Fig. S4G–H. **D.** Size exclusion chromatography of dynamin 1 oligomers. Dynamin 1 was mixed with either ATP or ATP with CSPα and Hsc70. The reaction mixtures were separated on a Superose 6 column and fractions were blotted for Dynamin 1 and CSPα. The curves show the average profile of dynamin 1 (n=3 independent experiments). Note that dynamin 1 shifts to a heavier molecular weight in the presence of Hsc70-CSPα. * = $p < 0.05$, ** = $p < 0.01$.

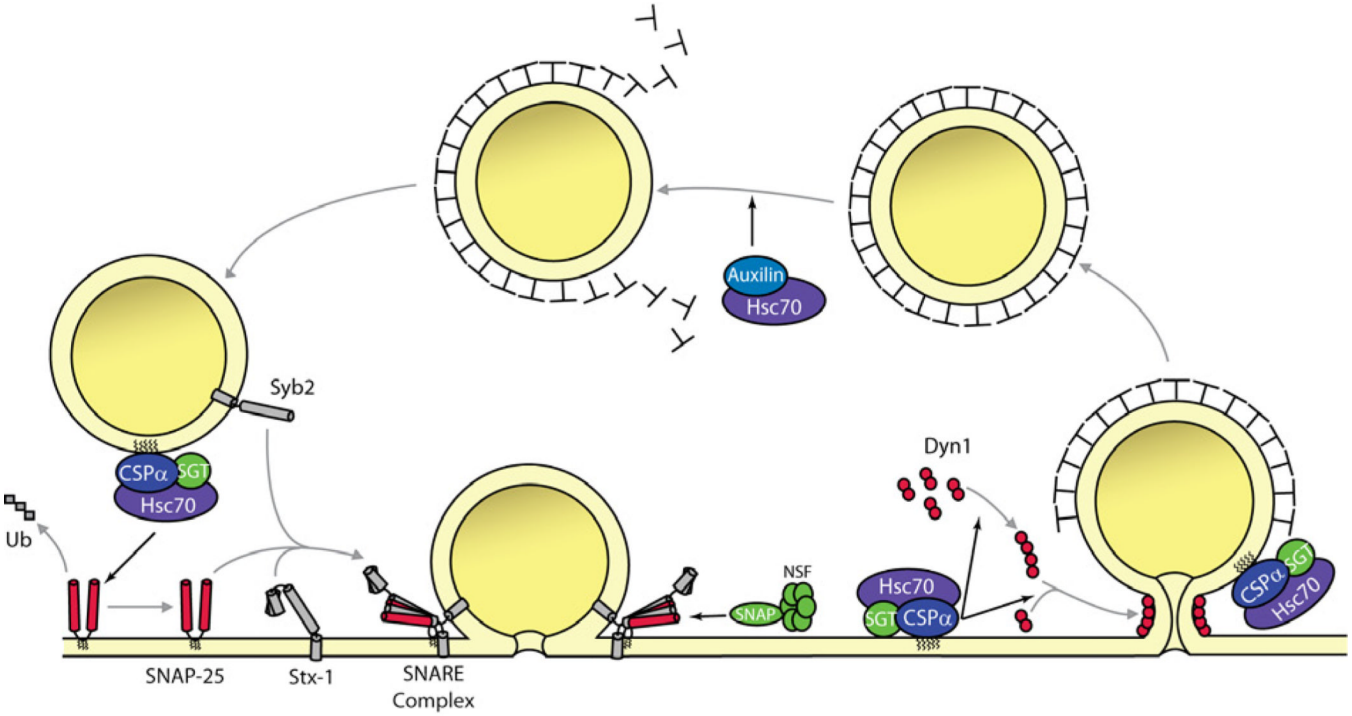

Figure 7. Model of CSPα function in the presynaptic terminal

CSPα recruits Hsc70 and SGT to form a functionally active chaperone complex on the synaptic vesicle. Hsc70-CSPα chaperone complex has two distinct functions at the presynaptic termini. First, Hsc70 binds unfolded SNAP-25 preventing its degradation. Lack of CSPα leads to decreased SNARE complex assembly and increased ubiquitination-dependent degradation of SNAP-25. Second, CSPα directly binds folded dynamin 1 and promotes its oligomerization, thereby facilitating synaptic vesicle endocytosis. Thus CSPα function may allow for efficient exo-endocytic coupling. How this results in structural stability of synapses remains to be identified. Also highlighted in the model are the other chaperones that function at other steps in the synaptic vesicle cycle, NSF, an AAA-ATPase that disassembles the SNARE complex and auxilin, that acts in clathrin uncoating. Thus chaperones are critical for the proper running of the synaptic vesicle cycle. Abbreviations: Stx-1, syntaxin 1a; Syb2, synaptobrevin 2; Dyn 1, dynamin 1; Ub, ubiquitin.

Table I

Proteins with decreased levels in CSPα KO synapses

Proteins exhibiting diminished levels in CSPα KO as compared to wildtype were identified either by DIGE or iTRAQ. As anticipated by the distinct chemistries of DIGE and iTRAQ, most proteins were identified by only one method, but several proteins were identified by both methods. Only those proteins that were decreased at least by 40% and found in multiple experiments are included. The entries are listed according to known function of the proteins and are ordered by the relative fold decrease in protein level. The number of peptides used to identify a given protein and the fraction in which the protein change was found are listed. Some of the proteins such as SNAP-25 were identified in several synaptic fractions. We validated the decreases in protein levels either by multiple reaction monitoring (MRM) or quantitative immunoblotting (WB). A '+' indicates a decrease in protein level was confirmed, a '−' no change in protein level was observed and 'NT' indicates not tested. For details of the MRM analysis, see Table S2. The functions of these proteins as defined by Gene Ontology were used to calculate probabilities of functions disrupted in CSPα KO synapses, see Table S1.

Protein ID	Gene	Protein Name	Fold Change	Method	Peptides	Fraction	Validated	Method
CHAPERONES								
IPI00875866	Dnajc5	CSPα	−4.18	iTRAQ	3	Vesicle/Memb	+	WB
IPI00330804	Hsp90aa1	Inducible Hsp90	−1.80	DIGE	34, 29	Cytosol	+	WB
IPI00229080	Hsp90ab1	Constitutive Hsp90	−1.80	DIGE	31–38	Cytosol	NT	
IPI00319992	Hspa5	Hsp70-5/GRP78	−1.78	DIGE	21	Membrane/Cytosol	+	MRM
IPI00123802	Hsph1	Hsp 105/110	−1.71	iTRAQ	5	Cytosol	NT	
IPI00323357	Hspa8	Hsc70	−1.67	DIGE/iTRAQ	21–33	Vesicle/Memb/Cytosol	+	MRM/WB
IPI00121514	Stip1	HOP	−1.54	DIGE	42,33	Cytosol	+	MRM/WB
IPI00317711	Hspa4l	Hsp70-4 like	−1.47	iTRAQ	7	Cytosol	NT	
IPI00116308	St13	Hip	−1.40	DIGE/iTRAQ	4	Cytosol	+	WB
IPI00116279	Cct5	Chaperonin TriC	−1.44	DIGE	20	Cytosol	+	MRM
EXOCYTOSIS								
IPI00125635	Snap25	SNAP-25b	−3.26	DIGE/iTRAQ	21–22	Vesicle/Memb/Cytosol	+	MRM/WB
IPI00626660	Cacnb4	Calcium channel β4	−1.64	iTRAQ	2	Membrane	NT	
IPI00656325	Nsf	NSF	−2.32	DIGE	7	Membrane	+	MRM/WB
IPI00132278	Cplx1	Complexin 1	−1.46	DIGE/iTRAQ	3, 7	Cytosol	+	WB
ENDOCYTOSIS								
IPI00845595	Dnm1	Dynamin 1	−2.44	DIGE	9–41	Vesicle/Memb	+	MRM/WB
IPI00225533	Necap1	Necap 1	−1.61	iTRAQ	4	Vesicle	+	MRM/WB
CYTOSKELETAL								

Protein ID	Gene	Protein Name	Fold Change	Method	Peptides	Fraction	Validated	Method
IPI00845581	Dpys14	Crmp3	−2.34	DIGE	14	Vesicle	−	MRM
IPI00808312	Sept3	Septin 3	−2.20	DIGE	7	Vesicle	+	MRM
IPI00850740	Sept5	Septin 5	−1.97	DIGE	15–22	Vesicle/Memb	−	MRM/WB
IPI00224626	Sept7	Septin 7	−1.90	DIGE	8–16	Vesicle	+	MRM
IPI00473707	Sept6	Septin 6	−1.64	DIGE	13	Vesicle	+	MRM
IPI00129519	Basp1	BASP1	−1.50	DIGE	3	Vesicle	+	WB
IPI00114375	Dpysl2	Crmp2	−1.41	DIGE	13	Cytosol	+	MRM
SIGNALING								
IPI00222430	Dbi	Diazepam binding inhib.	−2.00	iTRAQ	2	Vesicle	NT	
IPI00750256	Ak1	Adenylate kinase 1	−1.94	DIGE	6	Vesicle	+	MRM
IPI00227773	Ppp1cc	Protein phosphatase 1c	−1.68	iTRAQ	2	Vesicle	NT	
IPI00626797	Dlg4	PSD-95	−1.67	iTRAQ	2	Vesicle	−	MRM/WB
IPI00309207	Pafah1b1	PAFacetylhydrolase IBα	−1.60	iTRAQ	3	Vesicle	NT	
IPI00230418	Vsnl1	Visinin-like	−1.47	DIGE	16	Cytosol	+	MRM
IPI00653237	Wdr7	Rabconnectin 3β	−1.46	iTRAQ	1	Cytosol	−	MRM
IPI00761443	Iqsec1	ARF-GEP	−1.42	iTRAQ	1	Cytosol	+	MRM
OTHER								
IPI00331016	Sec24b	Sec24b	−2.44	iTRAQ	2	Vesicle	NT	
IPI00263013	Plp1	Proteolipid protein 1	−1.91	iTRAQ	6	Membrane	NT	
IPI00223377	Mbp	Myelin basic protein	−1.68	iTRAQ	13	Membrane	NT	
IPI00132734	Dynll2	Dynein light chain 2	−1.57	iTRAQ	5	Vesicle	NT	
IPI00845803	Snca	α-Synuclein	−1.49	DIGE/iTRAQ	3	Vesicle	+	MRM
IPI00131614	Sncb	β-Synuclein	−1.43	DIGE	8	Cytosol	+	MRM